Scientific paper

Fluoridobromate(V)-Hydrogen Fluoride Cocrystals

Martin Möbs¹,₀, Antti J. Karttunen² and Florian Kraus¹*₀

¹ Anorganische Chemie, Fluorchemie, Philipps-Universität Marburg, Hans-Meerwein-Str. 4, 35032 Marburg, Germany

² Department of Chemistry and Materials Science, Aalto University, 00076 Espoo, Finland

* Corresponding author: E-mail: f.kraus@uni-marburg.de Tel: +49 6421282666

Received: 04-09-2024

Dedicated to the late Prof. Dr. Boris Žemva

Abstract

Cocrystals of BrF₅ and HF₂⁻ salts have been obtained for the first time in the form of the two compounds [NMe₄] [(BrF₅)₆(HF₂)] and Cs₂[(BrF₅)₆(HF₂)(H₂F₃)]. These compounds are formed when hydrogen fluoride is present in reactions of BrF₅ and a fluoride ion source, such as [NMe₄]F or CsF. Here we present the crystal structures of the compounds, complemented by quantum chemical solid-state calculations, and our Raman spectroscopic investigations on the compound [NMe₄][(BrF₅)₆(HF₂)]. The cocrystals contain discrete [HF₂]⁻ and [H₂F₃]⁻ anions, which are coordinated by BrF₅ molecules via their F atoms. The propeller-like coordination of an F atom by three BrF₅ molecules, as known from the [Br₃F₁₆]⁻ anion, appears as a recurring structural motif in these compounds.

Keywords: Bromine pentafluoride; hydrogen fluoride; fluoridobromate(V); crystal structure; quantum chemical calculation; Raman spectroscopy.

1. Introduction

Seppelt and coworkers have reported the cocrystallization of iodine pentafluoride with fluoride ions and hydrogen fluoride. During their attempts to crystallize the $[IF_6]^-$ anion they obtained the compounds $Cs[HF_2] \cdot IF_5$, $NO[HF_2] \cdot IF_5$, $K[HF_2] \cdot 2IF_5$ and $Cs[H_3F_4] \cdot 3IF_5$, due to HF formation during the reactions or due to the usage of HF containing BrF_5 as a solvent. In the crystal structures of these compounds $[HF_2]^-$ or $[H_3F_4]^-$ ions act as bridging units between the iodine atoms of two or more IF_5 molecules, while the square pyramidal structure of the IF_5 molecules remains unchanged. IF_5

In reactions of bromine pentafluoride, BrF_5 , with a fluoride ion source such as CsF or $[NMe_4]F$, the fluoridobromate(V) anions $[BrF_6]^{-,2-5}$ $[Br_3F_{16}]^{-,6}$ or $[Br_4F_{21}]^{-}$ were obtained.⁷ In our attempts to obtain single crystals of such compounds, two unprecedented cocrystals of the BrF_5 and $[HF_2]^{-}$ or $[H_2F_3]^{-}$ molecules were observed, when no special care was taken to rigorously exclude HF from the reaction mixtures. Here we report the serendipitous synthesis of the compounds $[NMe_4][(BrF_5)_6(HF_2)]$ and $Cs_2[(BrF_5)_6(HF_2)(H_2F_3)]$ and their crystal structures.

2. Results and Discussion

2. 1. Synthesis and Crystal Structure of [NMe₄][(BrF₅)₆(HF₂)]

 $[NMe_4][(BrF_5)_6(HF_2)]$ was obtained in form of colorless crystals from a solution of $[NMe_4][HF_2]$ in BrF_5 upon cooling to -36 °C (see equation 1). The crystals liquefy when warmed up to room temperature.

$$[NMe_4][HF_2] + 6 BrF_5 \xrightarrow{BrF_5, -36 \, {}^{\circ}C} [NMe_4][(BrF_5)_6(HF_2)] (1)$$

The compound crystallizes in the monoclinic crystal system, space group C2/c (No. 15), with the lattice parameters $a=18.068(7),\ b=9.246(4),\ c=19.300(10)$ Å, $\beta=115.629(7)^\circ,\ V=2907.0(19)$ ų at 100 K with Z=4. Selected crystallographic data and details on the structure determination are given in Table 1 and in the Supporting Information (Tables S1-S5).

The $[(BrF_5)_6(HF_2)]^-$ anion is built up from a symmetrical, linear $[HF_2]^-$ anion, of which each of its F atoms is coordinated by three BrF_5 molecules in a pyramidal shape, as previously observed for the propeller shaped $[Br_3F_{16}]^-$ anion (Figure 1).⁶ The H atom resides at the in-

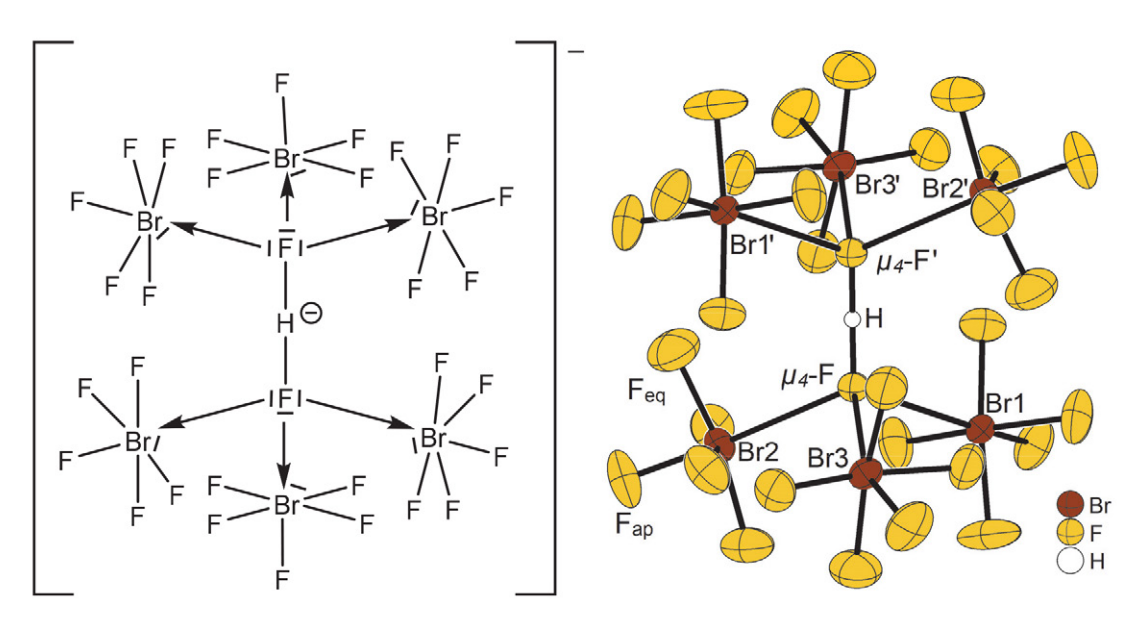


Figure 1. Structural formula (left) and section of the crystal structure of $[NMe_4][(BrF_5)_6(HF_2)]$ (right) showing the $[(BrF_5)_6(HF_2)]^-$ anion. Displacement ellipsoids are shown at 50% probability level at 100 K. [Symmetry codes: '3/2 - x, ½ - y, 1 - z]

version center of the unit cell (site symmetry $\bar{1}$, Wyckoff position 4c) while all other atoms reside on general positions.

The F···F distance in the $[HF_2]^-$ anion measures 2.265(4) Å, resulting in an intramolecular H–F distance of 1.1328(19) Å due to the inversion center of the anion. The F···F distance is the same within experimental error to that reported for $SrF[HF_2]$ with 2.269(6) Å, 8 it is slightly longer than the distance in the salt $[NMe_4][HF_2]$, which measures 2.213(4) Å, 9 and agrees within the tripled standard uncertainties to those in $Na[HF_2]$ and $K[HF_2]$, where the F···F distance is 2.277(1) Å and 2.277(6) Å, respectively. 10,11

In total, the [HF₂]⁻ anion is surrounded by six BrF₅ molecules in the shape of a trigonal antiprism. Each F atom of the [HF₂]⁻ anion is coordinated by three BrF₅ molecules in a trigonal pyramidal shape and thus is μ₄-bridging between one H and three Br atoms. The μ₄-F-Br distances are 2.660(2), 2.715(2) and 2.704(2) Å, which is longer than the reported μ_3 -F-Br distance in the $[Br_3F_{16}]^$ anion of 2.462(2) $Å^6$ and also longer than the μ_4 -F-Br distances in the $[Br_4F_{21}]^-$ anion of 2.474(3) and 2.5447(14) Å.⁷ The long μ_4 -F-Br distances in the $[(BrF_5)_6(HF_2)]^-$ anion can be interpreted as a result of the weaker ionic interaction between the [HF₂]- anion and the BrF₅ molecules compared to the stronger interaction of the mostly isolated fluoride ions with BrF5, as observed in the ions $[Br_3F_{16}]^-$ and $[Br_4F_{21}]^-$. The $Br-\mu_4$ -F-Br angles are 106.79(7)°, 105.61(7)°, and 106.18(7)°, resulting in a trigonal pyramidal arrangement of the three Br atoms and the μ_4 -F atom at the tip, with the μ_4 -F atom located 1.034(2) Å above the virtual plane spanned by the three Br atoms. The BrF₅ molecules are of regular square pyramidal shape and coordinate the μ_4 -F atom of the $[HF_2]$ -

anion via their free coordination site opposite from the apical F_{ap} atom. The μ_4 -F–Br– F_{ap} angles are 156.84(10) to 158.82(11)°. This deviation from 180° is due to the stereochemical activity of the free electron pair on the respective bromine atom, that was also observed for the $[Br_3F_{16}]^-$ and the $[Br_4F_{21}]^-$ anions. 6,7

The bond lengths and angles within the BrF $_5$ molecules are essentially the same as observed for the crystal structures of neat BrF $_5$. The equatorial Br-F $_{eq}$ and the apical Br-F $_{ap}$ bond lengths within the BrF $_5$ molecules of the $[(BrF_5)_6(HF_2)]^-$ anion range from 1.748(3) to 1.782(3)Å and 1.681(3) to 1.692(2) Å, respectively, while the Br-F distances in pure BrF $_5$ are 1.744(3) – 1.779(3) Å for the Br-F $_{eq}$ bonds and 1.686(2) Å for the Br-F $_{ap}$ bond. The F-Br-F angles in the coordinating BrF $_5$ molecules measure 83.70(13) – 84.87(15)° for the F $_{ap}$ -Br-F $_{eq}$ angles, 88.12(13) – 90.20(13)° for the F $_{eq}$ -Br-F $_{eq}$ angles between neighboring, and 167.88(13) – 169.41(14)° for the F $_{eq}$ -Br-F $_{eq}$ angles between opposing F $_{eq}$ atoms, and therefore are in accordance with those determined for neat BrF $_5$.

The [NMe₄]⁺ cation is located on the two-fold rotation axis (site symmetry 2, Wyckoff position 4e). Weak to moderate hydrogen bonds occur between the [NMe₄]⁺ cation and two F_{eq} atoms of a BrF₅ molecule with C···F hydrogen bond donor···acceptor distances of 3.153(7) and 3.310(12) Å. Further hydrogen bonds may occur but cannot be resolved due to a site disorder of the [NMe₄]⁺ ion. However, the H···F distances are overall in the proper range for C–H···F hydrogen bonds. 12

Each $[(BrF_5)_6(HF_2)]^-$ anion is octahedrally surrounded by six $[NMe_4]^+$ anions and *vice versa* resulting in the formation of two interpenetrating cubic closed packed sublattices (see Figure 2). Therefore, the packing of anions and cations resembles the one of the NaCl structure type.

Table 1. Selected crystallographic data and details of the structure determinations of $[NMe_4][(BrF_5)_6(HF_2)]$ and $Cs_2[(BrF_5)_6(HF_2)(H_2F_3)]$.

Compound	$[\mathrm{NMe_4}][(\mathrm{BrF_5})_6(\mathrm{HF_2})]$	Cs ₂ [(BrF ₅) ₆ (HF ₂)(H ₂ F ₃)] 1413.30	
Molar mass / g·mol ⁻¹	1162.61		
Space group (No.)	C2/c (15)	$P\bar{1}(2)$	
a / Å	18.068(7)	9.2987(6)	
b / Å	9.246(4)	9.5854(6)	
c / Å	19.300(10)	17.9037(10)	
α / °	90	92.778(5)	
β/°	115.629(7)	95.551(5)	
γ/°	90	118.596(4)	
V / ų	2907(2)	1386.33(15)	
Z	4	2	
Pearson symbol	mS224	aP92	
$\rho_{calc.}$ / g·cm ⁻³	2.656	3.385	
μ / mm ⁻¹	8.494	11.507	
Color	colorless	colorless	
Crystal morphology	block	block	
Crystal size / mm ³	$0.267 \times 0.134 \times 0.063$	$0.245 \times 0.209 \times 0.078$	
T/K	100	100	
λ/Å	$0.71073 (Mo-K_a)$	$0.71073 (Mo-K_a)$	
No. of reflections	15327	18042	
θ range / °	2.533 - 27.172	2.299 - 26.727	
Range of Miller indices	$-23 \le h \le 23$	$-10 \le h \le 11$	
Č	$-11 \le k \le 11$	$-12 \le k \le 12$	
	$-24 \le l \le 23$	$-22 \le l \le 22$	
Absorption correction	numerical	numerical	
T_{\max} , T_{\min}	0.8757, 0.3562	0.2475, 0.1029	
$R_{\rm int}, R_{\sigma}$	0.0418, 0.0321	0.0820, 0.0584	
Completeness of the data set	0.997	1	
No. of unique reflections	3190	5885	
No. of parameters, restraints, constraints	209, 6, 0	401, 0, 0	
S (all data)	1.038	1.030	
$R(F)$ ($I \ge 2\sigma(I)$, all data)	0.0299, 0.0407	0.0397, 0.0602	
$wR(F^2)$ ($I \ge 2\sigma(I)$, all data)	0.0667, 0.0700	0.0892, 0.0974	
Extinction coefficient	_	0.00103(14)	
$\Delta \rho_{max}$, $\Delta \rho_{min}$ / e ·Å ⁻³	0.854, -0.527	0.775, -1.711	

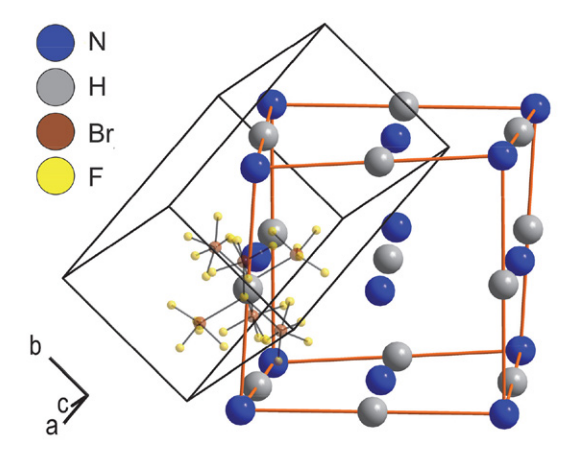


Figure 2. Section of the crystal structure of $[NMe_4][(BrF_5)_6(HF_2)]$ with the monoclinic unit cell in black. The nitrogen atoms (blue spheres) and hydrogen atoms (gray spheres) form the centers of gravity of the $[NMe_4]^+$ cations and the $[(BrF_5)_6(HF_2)]$ anions, respectively. Their arrangement shows the structural relation to the NaCl structure type with the pseudo cubic unit cell in orange. A $[(BrF_5)_6(HF_2)]^-$ anion is shown transparently in the ball and stick model. Atoms are shown with arbitrary radii.

2. 2. Synthesis and Crystal Structure of $Cs_2[(BrF_5)_6(HF_2)(H_2F_3)]$

Colorless crystals of $Cs_2[(BrF_5)_6(HF_2)(H_2F_3)]$ were obtained from a solution of CsF dissolved in BrF₅ that adventitiously contained HF upon cooling to -36 °C (equation 2).

$$2 \text{ CsF} + 6 \text{ BrF}_5 + 3 \text{ HF} \xrightarrow{\text{BrF}_5, -36 \text{ °C}} \\
\text{Cs}_2[(\text{BrF}_5)_6(\text{HF}_2)(\text{H}_2\text{F}_3)]$$
(2)

The crystals liquefy quickly at room temperature. If pure BrF₅ is used, the compound Cs[Br₃F₁₆] is obtained under otherwise exactly the same conditions. Cs₂[(BrF₅)₆(HF₂)(H₂F₃)] crystallizes in the triclinic crystal system, space group $P\bar{1}$ (No. 2), with the lattice parameters $a=9.2987(6),\ b=9.5854(6),\ c=17.9037(10)$ Å, $\alpha=92.778(5),\ \beta=95.551(5)^{\circ},\ \gamma=118.596(4)^{\circ},\ V=1386.33(15)$ ų at 100 K with Z=2. Selected crystallographic data and details on the structure determination

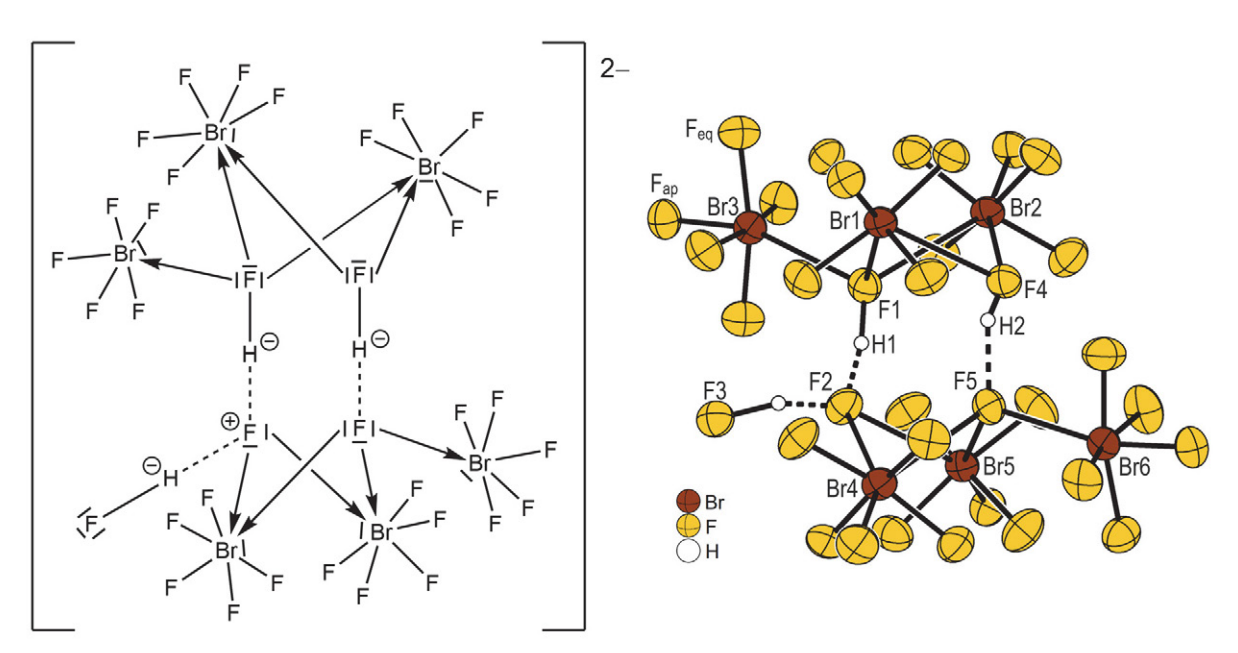


Figure 3. Structural formula (left) and section of the crystal structure of $Cs_2[(BrF_5)_6(HF_2)(H_2F_3)]$ (right) showing the $[(BrF_5)_6(HF_2)(H_2F_3)]^-$ anion. Displacement ellipsoids are shown at 50% probability level at 100 K.

are given in Table 1 and in the Supporting Information (Tables S6-S10).

The $[(BrF_5)_6(HF_2)(H_2F_3)]^-$ anion consists of $[H_2F_3]^-$ and a $[HF_2]^-$ anion which are connected by six BrF_5 molecules as shown in Figure 3.

The F1-F2-F3 angle of the $[H_2F_3]$ anion is 105.6(2)°. This is relatively small due to the sterical influence of the coordinating BrF₅ molecules. For comparison, in Cs[H₂F₃] the F...µ-F...F angles are much larger measuring 148.4(6) and 141.2(6)°.13 However, the counter cations have an influence and the bond angles shrink with increasing cation-anion interaction. Therefore, the F---u-F---F angles in Rb[H₂F₃] measure 145.5(3) and 136.4(3)°, 14 139.2(9) and $129.8(7)^{\circ}$ in K[H₂F₃], ¹⁵ and $115.58(5)^{\circ}$ in Na[H₂F₃]. ¹⁶ When even stronger cation...anion interaction, such as hydrogen bonding, is present, the F...µ-F...F angle can become even smaller, as observed in [HNMe₃][H₂F₃] with a F···μ-F···F angle of 97.9(1)°. 17 The F1···F2 and the F2···F3 distance are 2.304(5) and 2.363(6) Å, respectively, which is within the typical range of common [H₂F₃]⁻ compounds.¹³⁻¹⁶ The H-F bond lengths of 1.10(10) and 1.19(15) Å and the H···μ-F distances of 1.22(10) and 1.22(15) Å are the same within the tripled standard uncertainty and it is thus not clear if a symmetric or an unsymmetric hydrogen bond is present. The F-H···u-F angles are 166(9) and 158(13)°. Overall, the short F...F distances indicate that strong hydrogen bonds¹⁸ are present.

The $[HF_2]^-$ ion in the crystal structure of $Cs_2[(BrF_5)_6(HF_2)(H_2F_3)]$ is asymmetric with F4–H2 and F5···H2 distances of 0.80(9) and 1.58(10) Å, respectively, while the F4–H2····F5 angle is 155(11)°. The F4–F5 distance of 2.321(5) Å is slightly longer than the one observed in $[NMe_4][(BrF_5)_6(HF_2)]$ indicating a weaker hydrogen bond

which is in accordance with the F4–H2···F5 angle deviating from 180°.

The F1 atom belonging to the $[H_2F_3]^-$ anion is coordinated by three BrF₅ molecules via the bromine atoms Br1, Br2 and Br3 in a trigonal pyramidal arrangement, similar as observed in the compound Cs[Br₃F₁₆].⁶ The Br1-3–F1 distances, however, are notably longer with 2.798(4), 2.925(4), and 2.664(4) Å compared to the one observed in Cs[Br₃F₁₆] measuring 2.462(2) Å. Additionally, the bromine atoms Br1 and Br2 are both connected to the F4 atom oft $[HF_2]^-$ anion with Br1-2–F4 distances of 2.808(4) and 2.841(4) Å. Thus, the fluoridobromate anion is not considered as a $[Br_3F_{16}]^-$ anion, but the coordination of another fluoride ion results in the formal formation of a $[Br_3F_{17}]^{2-}$ moiety, if the hydrogen atoms are disregarded (see Figure 4a).

The same applies for the bromine atoms Br4, Br5, and Br6 which are involved in the coordination of the F5 atom of $[HF_2]^-$ anion, again in a trigonal pyramidal arrangement. Br4-6–F5 distances are equal to 2.790(4), 2.714(4), and 2.529(4) Å. The Br4 and Br5 atoms are additionally involved in the coordination sphere of the neighboring the $[H_2F_3]^-$ anion with Br4-5–F2 distances of 2.739(4) and 2.857(4) Å, respectively. Thus, the arrangement of the bromine atoms Br4, Br5, and Br6 also results in the formal formation of a $[Br_3F_{17}]^{2-}$ moiety. Alternatively, the sum formula of the compound can therefore be rewritten as $Cs_2[H_2(Br_3F_{17})_2]$ ·HF.

Within the two $[Br_3F_{17}]^{2-}$ anions the bromine atoms Br1, Br2, Br4, and Br5 are coordinated sevenfold by F atoms in the shape of a capped trigonal prism (see Figure 4b) while the Br3 and the Br6 atom are coordinated sixfold by F atoms in the shape of a distorted octahedron (see Figure 4c).

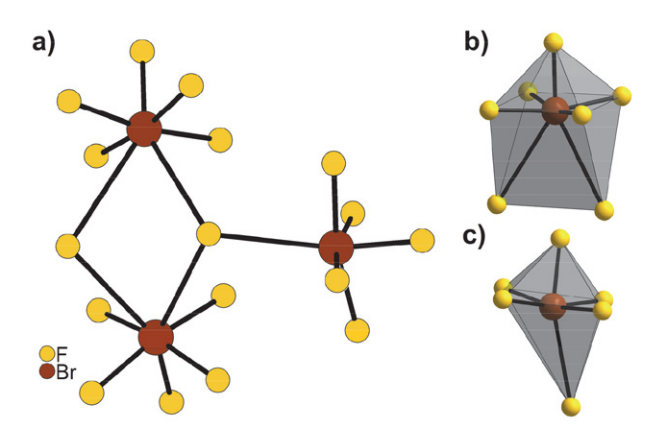


Figure 4. a) Section of the crystal structure of $Cs_2[(BrF_5)_6(HF_2)]$ (H_2F_3)] showing the interconnection of three BrF_5 moieties bridged by two fluoride ions resulting in the virtual $[Br_3F_{17}]^{2-}$ anion. Therein the Br atoms are either coordinated sevenfold in the shape of a capped trigonal prism (b) or sixfold with a distorted octahedral shape (c). Atoms are shown as spheres with arbitrary radii.

Bond lengths and angles observed for the coordinating BrF₅ molecules are similar to those determined for pure BrF₅. The lengths of the apical Br–F_{ap} bonds range from 1.689(4) to 1.702(4) Å, the equatorial Br–F_{eq} bond lengths range from 1.747(4) to 1.797(4) Å. For comparison, the Br–F distances in neat BrF₅ are 1.686(2) Å for the Br–F_{ap} bond and 1.744(3)– 1.779(3) Å for the Br–F_{eq} bonds.⁵ The F_{ap}–Br–F_{eq} angles in the crystal structure of Cs₂[(BrF₅)₆(HF₂)(H₂F₃)] are in the range of 83.54(17) to 85.0(2)°. The F_{eq}–Br–F_{eq} angles between two neighboring fluorine atoms are in the range from 88.5(3) to 90.1(3)°.

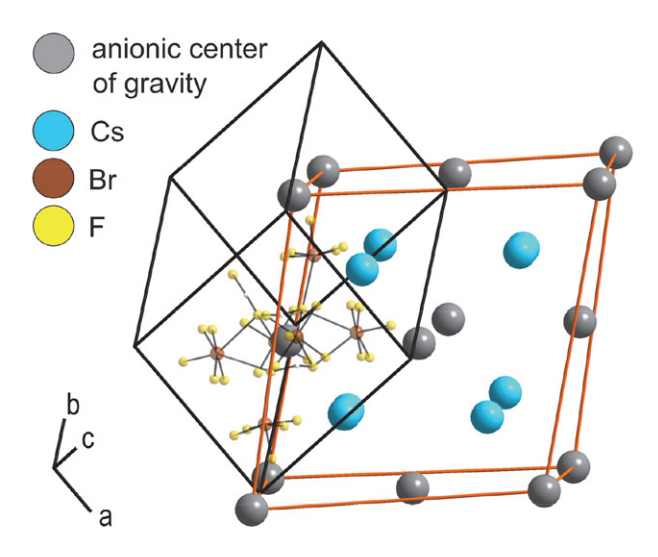


Figure 5. Section of the crystal structure of $Cs_2[(BrF_5)_6(HF_2)(H_2F_3)]$ with the triclinic unit cell in black. The arrangement of the Cs cations (sky blue spheres) and the centers of gravity of the $[(BrF_5)_6(HF_2)(H_2F_3)]^{2-}$ anions (gray spheres) illustrates the structural relationship to the inverse CaF_2 structure type with the pseudo cubic unit cell in orange. A $[(BrF_5)_6(HF_2)(H_2F_3)]^{2-}$ anion is shown transparently in the ball and stick model. Atoms are shown with arbitrary radii.

In the crystal structure of $Cs_2[(BrF_5)_6(HF_2)(H_2F_3)]$ each $[(BrF_5)_6(HF_2)(H_2F_3)]^{2-}$ anion is surrounded by eight Cs^+ cations in a distorted cubic shape, while the Cs^+ cations are surrounded in a tetrahedron-like shape by the $[(BrF_5)_6(HF_2)(H_2F_3)]^{2-}$ anions. The structure can therefore be traced back to the inverse CaF_2 structure type, that is, the Li_2O structure type. The structural relationship becomes apparent when the positions of the centers of gravity of the anions are drawn as shown in Figure 5.

2. 3. Quantum-Chemical Calculations

The crystal structures of [NMe₄][(BrF₅)₆(HF₂)] and $Cs_2[(BrF_5)_6(HF_2)(H_2F_3)]$ have been quantum-chemically optimized in terms of lattice parameters and atomic positions using hybrid density functional methods (DFT-PBE0-TZVP/SVP level of theory, see experimental section for additional computational details). The optimized structures have been confirmed as true local minima on the potential energy surface by harmonic frequency calculation. The largest deviation of the optimized lattice parameters from the lattice parameters determined by X-ray diffraction is 3.4 % for the compound [NMe₄] $[(BrF_5)_6(HF_2)]$ and 1.4 % for $Cs_2[(BrF_5)_6(HF_2)(H_2F_3)]$. A comparison of the measured and calculated lattice parameters is given in Table 2. Atom positions, bond lengths and angles of the optimized structure are in overall agreement with those determined experimentally. A visual comparison for both of the crystal structures and a tabularly comparison of selected interatomic distances and angles are given in the Supporting information (Figures S1-2, Tables S3-4, S8-9, optimized structures in CIF format p. S11-13).

2. 4. Raman Spectroscopy

A Raman spectrum was recorded on a cluster of randomly orientated crystals of $[NMe_4][(BrF_5)_6(HF_2)]$ immersed in perfluoropolyether oil cooled to -60 °C. However, a spectrum of $Cs_2[[(BrF_5)_6(HF_2)(H_2F_3)]$ could not be recorded due to ice formation and rapid decomposition of the compound during the attempted measurement. Raman spectra of both compounds have been calculated on the basis of the quantum-chemically optimized solid-state structures. A comparison of the observed and calculated Raman spectra of $[NMe_4][(BrF_5)_6(HF_2)]$ is shown in Figure 6. The calculated spectrum for $Cs_2[(BrF_5)_6(HF_2)(H_2F_3)]$ and the band assignments for the spectra of both compounds are given in the Supporting Information (Figure S3, Table S11).

Raman bands in the region above $700~\rm cm^{-1}$ belong to the [NMe₄]⁺ cation, bands below $700~\rm cm^{-1}$ can be assigned to the BrF₅ molecules. The bands from 685 to 529 cm⁻¹ originate from stretching vibrations of Br-F_{eq} and Br-F_{ap} bonds, while those from 434 – 239 cm⁻¹ can be attributed to deformation vibrations of the BrF₅ molecules. The Raman active stretching vibrations of the [HF₂]⁻ anion al-

Table 2. Comparison of experimentally determined lattice parameters of $[NMe_4][(BrF_5)_6(HF_2)]$ and $Cs_2[(BrF_5)_6(HF_2)(H_2F_3)]$ with the results of the DFT structure optimization (DFT-PBE0-TZVP/SVP).

	[NMe4][(BrF5)6(HF2)]			$Cs_2[(BrF_5)_6(HF_2)(H_2F_3)]$		
	Experiment	DFT	Difference Δ / %	Experiment	DFT	Difference Δ / %
a / Å	18.068(7)	18.1542	0.5	9.2987(6)	9.4293	1.4
<i>b</i> / Å	9.246(4)	9.2008	0.5	9.5854(6)	9.6942	1.1
c / Å	19.300(10)	19.9528	3.4	17.9037(10)	18.0875	1.0
α/°	90	90	_	92.778(5)	92.6564	0.1
β/°	115.629(7)	114.1183	1.3	95.551(5)	95.2156	0.4
γ/°	90	90	_	118.596(4)	118.7920	0.2

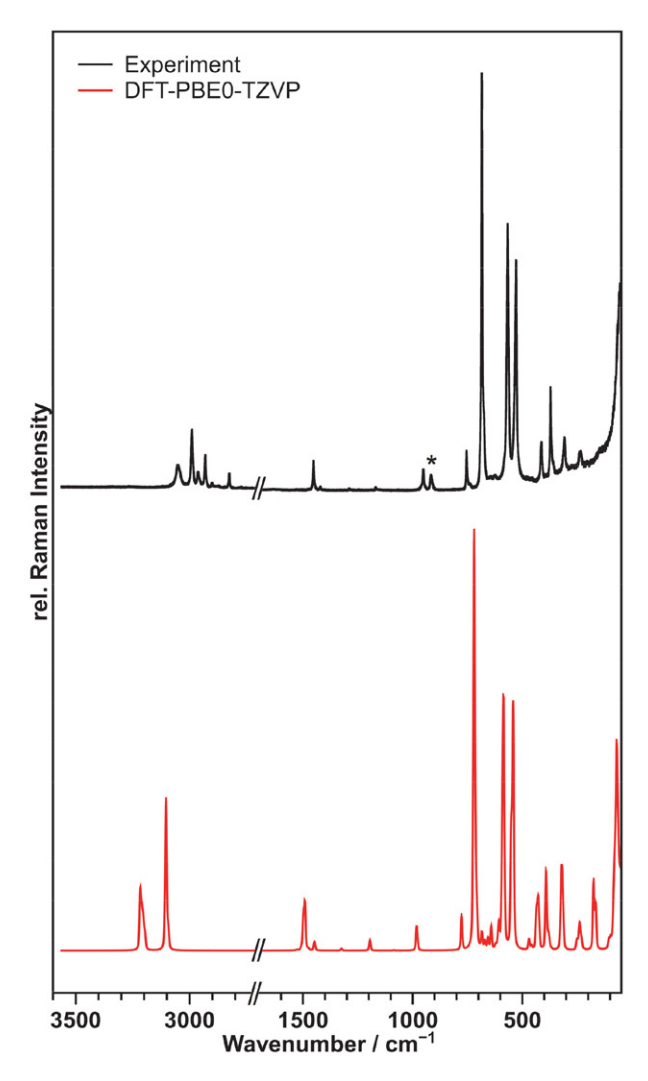


Figure 6. Observed Raman spectrum of [NMe₄][(BrF₅)₆(HF₂)] suspended in perfluoropolyether oil at -60 °C (black trace) compared to the calculated spectrum at the DFT-PBE0/TZVP level of theory (red trace). No bands were observed or calculated in the range from $1700-2700~\text{cm}^{-1}$ so it was omitted from the figure. The band marked with an asterisk originates from BrO₂F, which is a hydrolysis product formed during the Raman measurement.¹⁹

ways occur in combination with either deformation vibrations of the methyl groups, at 1448 cm⁻¹, or Br–F stretching vibrations, at 625 and 566 cm⁻¹. Therefore the observed

Raman spectrum is dominated by the bands of the $[NMe_4]^+$ cation and the BrF_5 molecules and thus looks very similar to the spectrum of $[NMe_4][Br_4F_{21}]$ that was recently reported.⁷

The observed spectrum is reproduced by the calculation, with only a few exceptions: The calculated frequencies are slightly overestimated as anharmonic effects have not been considered in the frequency calculation.² The additional bands in the region of 2826 to 2962 cm⁻¹, can be assigned to combination bands of the [NMe₄]⁺ ion and therefore are not predicted by the calculation.^{21,22} The additional band marked with an asterisk at 912 cm⁻¹ is due to an impurity of BrO₂F, which is a hydrolysis product of BrF₅.¹⁹

3. Conclusions

This study presents the successful synthesis of BrF₅ and HF₂⁻ salt cocrystals, exemplified by the compounds $[NMe_4][(BrF_5)_6(HF_2)]$ and $Cs_2[(BrF_5)_6(HF_2)(H_2F_3)]$. Our results show a preferential formation of such cocrystals in the presence of HF, whereas the previously known fluoridobromate(V) compounds Cs[Br₃F₁₆] and [NMe₄][Br₄F₂₁] are formed only under rigorous exclusion of HF, but otherwise under the same conditions. The X-Ray crystal structures of the compounds [NMe₄][(BrF₅)₆(HF₂)] and $Cs_2[(BrF_5)_6(HF_2)(H_2F_3)]$ reveal the coordination of the F atoms of the [HF₂]⁻ or [H₂F₃]⁻ anions, respectively, by BrF₅ molecules. This results in the formal formation of two virtual fluoridobromate(V) anions: the previously known μ₃-bridged [Br₃F₁₆]⁻ anion and the newly discovered [Br₃F₁₇]²⁻ anion, which is derived from the latter by the formal addition of another fluoride ion bridging two Br atoms. In addition, our crystal structure elucidation was validated and complemented by quantum chemical solid-state calculations. The recorded Raman spectrum for [NMe₄][(BrF₅)₆(HF₂)] confirms our structural findings and provides experimental confirmation of the calculated spectrum.

Conflict of interest

The authors declare no conflicts of interest.

4. Experimental

General: All operations were performed on a Monel steel Schlenk line, which was passivated with fluorine at various temperatures and pressures before use. Reaction vessels were made out of fluoropolymer (perfluoroalkoxy alkanes, PFA) and sealed with a PFA needle valve (Swagelok). The vessels were baked out in vacuum ($\sim 10^{-3}$ mbar) at circa 100 °C for several times and passivated with diluted F₂ (F₂/Ar 20:80, v/v, Solvay). CsF was purchased from Merck and purified according to literature methods.²³ [NMe₄]F or [NMe₄][HF₂] was taken from the laboratory stock. Solid starting materials were stored and handled in an Ar-filled (Ar 5.0, Nippon Gases) glove box (MBraun). BrF₅ was prepared according to the literature.⁵

Caution! F₂, BrF₅, and HF are highly toxic, strong oxidizers, or both. Therefore, proper protective equipment must be worn, and appropriate emergency treatment procedures must be available in case of contact. F₂ or BrF₅ may react explosively with organic material, such as organic solvents or [NMe₄]⁺ salts. It is crucial to take the utmost precautions when handling or disposing of these materials and their derivatives.

Synthesis of $[NMe_4][(BrF_5)_6(HF_2)]$: 63 mg (0.56 mmol) $[NMe_4][HF_2]$ was loaded into a PFA reaction vessel inside the glove box and an excess of BrF_5 (0.62 mL, 8.7 mmol) was distilled onto the solid at -196 °C. The reaction mixture was allowed to warm up to room temperature giving a colorless solution. Cooling the reaction mixture to -36 °C for several hours led to the formation of colorless crystals of $[NMe_4][(BrF_5)_6(HF_2)]$.

It should be noted, that the reaction attempted was that of [NMe₄]F and BrF₅. However, the [NMe₄]F taken from the laboratory stock turned out to contain significant amounts of [NMe₄][HF₂], as shown by ¹H and ¹⁹F NMR spectroscopy (see S.I. p. S19 for further details).

Synthesis of $Cs_2[(BrF_5)_6(HF_2)(H_2F_3)]$: 45 mg (0.30 mmol) CsF was loaded into a PFA reaction vessel inside the glove box and an excess of HF-containing BrF₅ (0.50 mL, 7.0 mmol) was distilled onto the solid at –196 °C. The reaction mixture was allowed to warm up to room temperature giving a colorless solution with some undissolved colorless solid remaining. Cooling the reaction mixture to –36 °C for several hours led to the formation of colorless crystals of $Cs_2[(BrF_5)_6(HF_2)(H_2F_3)]$.

Nota bene: In order to avoid HF contamination in BrF_5 , it should be stored over KF, which was not done in this case. KF removes traces of HF by forming K[HF₂]. If PFA vessels are used to store BrF_5 , it should be stored at low temperature and at an overpressure of additionally added F₂ or F₂/Ar inside the vessel to counteract the diffusion of water and other contaminants through the fluoropolymer.

4. 1. Crystal Structure Determination

Crystals of the compounds $[NMe_4][(BrF_5)_6(HF_2)]$ and $Cs_2[(BrF_5)_6(HF_2)(H_2F_3)]$ were transferred from BrF_5

solution, cooled to -40 °C, in into pre-cooled perfluoro-polyether oil (Galden LS\230, Solvay, stored over molecular sieves 3 Å). Suitable crystals were selected in absence of air under the microscope and mounted on a MiTeGen loop.

Intensity data for the compound [NMe₄][(BrF₅)₆ (HF₂)] was recorded with a Bruker Quest D8 diffractometer. The diffractometer was operated with monochromatized Mo-K α radiation (0.71073 Å, multi layered optics) and equipped with a PHOTON 100 CMOS detector. Evaluation, integration, and reduction of the diffraction data was carried out with the APEX3 software suite.²⁴ A numerical absorption correction was applied using the SADABS program implemented in the APEX3 software.²⁵

Intensity data of a suitable crystal of $Cs_2[(BrF_5)_6(HF_2)$ $(H_2F_3)]$ was recorded with an IPDS2 diffractometer (Stoe & Cie). The diffractometer was operated with Mo-K α radiation (0.71073 Å, graphite monochromator) and equipped with an image plate detector. Evaluation, integration and reduction of the diffraction data was carried out using the X-Area software suite. A numerical absorption correction was applied with the modules X-Shape and X-Red32 of the X-Area software suite.

The structures were solved with dual-space methods (SHELXT) and refined against F^2 (SHELXL). ^{27,28} All non-hydrogen atoms were refined with anisotropic displacement parameters. Hydrogen atom positions, except the ones of the [NMe₄]⁺ ion, were located from the electron density difference map and the H-atom positions and isotropic displacement parameters were refined freely. H atom positions of the disordered methyl groups were calculated and refined using a riding model (AFIX) with isotropic displacement parameters 1.5 times U_{eq} of the associated carbon atom.

Representations of the crystal structures were created with the Diamond,²⁹ or the VESTA³⁰ software. CCDC 2345883 and 2345884 contain the supplementary crystallographic data for this paper. These data are provided free of charge by The Cambridge Crystallographic Data Centre.

4. 2. Raman Spectroscopy

The Raman spectrum was measured with a Monovista CRS+ confocal Raman microscope (Spectroscopy & Imaging GmbH) using a 532 nm solid-state laser and either a 300 grooves/mm (low-resolution mode, FWHM: <4.62 cm⁻¹) or an 1800 grooves/mm (high -resolution mode, FWHM: <0.368 cm⁻¹) grating. Sample preparation of [NMe₄][(BrF₅)₆(HF₂)]: Crystals of the compound were selected in the absence of air under dried, cooled perfluoropolyether oil (Galden LS\230, Solvay, stored over molecular sieves 3 Å) using an optical microscope. For the transfer to the Raman microscope, crystals were cooled with liquid nitrogen and then placed inside a pre-cooled sample cell (BCS196, Linkam) on the microscopy stage of

the Raman microscope. The time of contact with the air was kept as short as possible. The spectrum was recorded at -60 °C.

4. 3. Quantum Chemical Details

Solid-state calculations on the compounds [NMe₄] $[(BrF_5)_6(HF_2)]$ and $Cs_2[(BrF_5)_6(HF_2)(H_2F_3)]$ were performed with the CRYSTAL23³¹ program suite using hybrid density functional methods (DFT-PBE0)32,33 combined with triple-valence + polarization (TZVP) basis sets for C, H, N, Br and F atoms 34-36 and a split-valence + polarization (SVP) basis set for the Cs atoms.³⁷ Additional details on the basis sets are given in the Supporting Information (p. S9-10). Atomic positions and lattice parameters were fully optimized within the space group symmetry. The reciprocal space was sampled with a 3×3×2 Monkhorst-Pack-type³⁸ k-point grid for both structures, [NMe₄] $[(BrF_5)_6(HF_2)]$ and $Cs_2[(BrF_5)_6(HF_2)(H_2F_3)]$. Tight truncation criteria (TOLINTEG 8, 8, 8, 8, 16) were applied for the evaluation of the bielectronic Coulomb and exchange series in all calculations. Default DFT integration grids and optimization convergence thresholds were used in all calculations. Harmonic vibrational frequencies and Raman intensities were calculated with the schemes implemented in CRYSTAL.³⁹⁻⁴¹ The harmonic frequencies confirmed the optimized structures as true local minima. Raman intensities were calculated for a polycrystalline powder sample, applying the same conditions as in the experimental setup (T = 213.15 K and $\lambda = 532$ nm). For the simulation of the Raman spectrum, a pseudo-Voigt band profile (50:50 Lorentzian:Gaussian) with a FWHM of 8 cm⁻¹ was used. Assignment of the vibrational bands was done with the visualization tool CRYSPLOT⁴².

Acknowledgement

We thank Solvay for the kind donations of fluorine.

5. References

- A. R. Mahjoub, D. Leopold, K. Seppelt, Eur. J. Solid State Inorg. Chem. 1992, 29, 635–648.
- A. R. Mahjoub, A. Hoser, J. Fuchs, K. Seppelt, *Angew. Chem.*, Int. Ed. 1989, 28, 1526–1527. DOI:10.1002/anie.198915261
- 3. A. R. Mahjoub, X. Zhang, K. Seppelt, *Chem. Eur. J.* **1995**, *1*, 261–265. **DOI**:10.1002/chem.19950010410
- R. Bougon, P. Charpin, J. Soriano, C. R. Acad. Sc. Paris, Ser. C 1971, 272, 565–568.
- M. Möbs, T. Graubner, K. Eklund, A. J. Karttunen, F. Kraus, *Chem. - Eur. J.* 2022, 28, e202202466. DOI:10.1002/chem.202202466
- M. Möbs, T. Graubner, A. J. Karttunen, F. Kraus, *Chem. Eur. J.* 2023, 29, e202301876.
- 7. M. Möbs, T. Graubner, A. J. Karttunen, F. Kraus, Chem. Sci.

- 2024, 15, 3273-3278. DOI:10.1039/D3SC06688F
- W. Massa, E. Herdtweck, Acta Crystallogr., Sect. C: Cryst. Struct. Commun. 1983, 39, 509–512.
 DOI:10.1107/S0108270183005314
- 9. W. W. Wilson, K. O. Christe, J. Feng, R. Bau, *Can. J. Chem.* **1989**, *67*, 1898–1901. **DOI:**10.1139/v89-295
- 10. A. M. Panich, *Chem. Phys.* **1995**, *196*, 511–519. **DOI:**10.1016/0301-0104(95)00128-B
- J. A. Ibers, J. Chem. Phys. 1964, 40, 402–404.
 DOI:10.1063/1.1725126
- E. D'Oria, J. J. Novoa, CrystEngComm 2008, 10, 423–436.
 DOI:10.1039/b717276c
- S. I. Troyanov, I. V. Morozov, E. Kemnitz, Z. Anorg. Allg. Chem. 2005, 631, 1651–1654.
 DOI:10.1002/zaac.200500071
- 14. M. Möbs, Untersuchungen zur Photochemie von Fluor und seinen Verbindungen, Master Thesis, Philipps-Universität Marburg, 2020.
- J. D. Forrester, M. E. Senko, A. Zalkin, D. Templeton, Acta Crystallogr. 1963, 16, 58–62.

DOI:10.1107/S0365110X63000098

- S. I. Ivlev, T. Soltner, A. J. Karttunen, M. J. Mühlbauer, A. J. Kornath, F. Kraus, Z. Anorg. Allg. Chem. 2017, 643, 1436–1443. DOI:10.1002/zaac.201700228
- D. Wiechert, D. Mootz, R. Franz, G. Siegemund, *Chem. Eur. J.* 1998, 4, 1043–1047.
 DOI:10.1002/(SICI)1521-3765(19980615)4:6<1043::AID-CHEM1043>3.0.CO;2-N
- 18. G. A. Jeffrey, *An Introduction to Hydrogen Bonding*, Oxford University Press, **1997**.
- R. J. Gillespie, P. H. Spekkens, J. Chem. Soc., Dalton Trans. 1977, 1539–1546. DOI:10.1039/dt9770001539
- J. P. Merrick, D. Moran, L. Radom, J. Phys. Chem. A 2007, 111, 11683–11700. DOI:10.1021/jp073974n
- 21. G. Kabisch, *J. Raman Spectrosc.* **1980**, *9*, 279–285. **DOI:**10.1002/jrs.1250090502
- 22. G. Kabisch, M. Klose, *J. Raman Spectrosc.* **1978**, *7*, 311–315. **DOI:**10.1002/jrs.1250070604
- 23. G. Brauer, *Handbuch der präparativen anorganischen Chemie in drei Bänden*, Ferdinand Enke Verlag, Stuttgart, **1975**.
- 24. *APEX3 V2019.11-2*, Bruker AXS Inc., Madison, Wisconsin, USA, **2019**.
- 25. SADABS, Bruker AXS Inc., Madison, Wisconsin, USA, 2016.
- 26. X-Area 1.8.1, STOE & Cie GmbH, Darmstadt, Germany, 2018.
- 27. G. M. Sheldrick, *Acta Crystallogr.* **2015**, *A71*, 3–8. **DOI:**10.1107/S2053273314026370
- 28. G. M. Sheldrick, SHELXL-2016/6, Göttingen, Germany, 2016.
- 29. K. Brandenburg, H. Putz, Diamond Crystal and Molecular Structure Visualization, V 4.6.8, Crystal Impact GbR, Bonn, 2022.
- K. Momma, F. Izumi, J. Appl. Crystallogr. 2011, 44, 1272– 1276. DOI:10.1107/S0021889811038970
- A. Erba, J. K. Desmarais, S. Casassa, B. Civalleri, L. Donà, I.
 J. Bush, B. Searle, L. Maschio, L. Edith-Daga, A. Cossard, C.

- Ribaldone, E. Ascrizzi, N. L. Marana, J.-P. Flament, B. Kirtman, *J. Chem. Theory Comput.* **2023**, *19*, 6891–6932. **DOI:**10.1021/acs.jctc.2c00958
- J. P. Perdew, K. Burke, M. Ernzerhof, *Phys. Rev. Lett.* 1996, 77, 3865–3868. DOI:10.1103/PhysRevLett.77.3865
- C. Adamo, V. Barone, J. Chem. Phys. 1999, 110, 6158–6170.
 DOI:10.1063/1.478522
- S. I. Ivlev, K. Gaul, M. Chen, A. J. Karttunen, R. Berger, F. Kraus, *Chem. Eur. J.* 2019, 25, 5793–5802.
 DOI:10.1002/chem.201900442
- A. J. Karttunen, T. Tynell, M. Karppinen, J. Phys. Chem. C
 2015, 119, 13105–13114. DOI:10.1021/acs.jpcc.5b03433
- S. S. Rudel, T. Graubner, A. J. Karttunen, F. Kraus, Z. Anorg. Allg. Chem. 2020, 646, 1396–1402.
- R. E. Stene, B. Scheibe, A. J. Karttunen, W. Petry, F. Kraus, Eur. J. Inorg. Chem. 2019, 2019, 3672–3682.
 DOI:10.1002/ejic.201900595

- H. J. Monkhorst, J. D. Pack, *Phys. Rev. B* 1976, 13, 5188–5192.
 DOI:10.1103/PhysRevB.13.5188
- L. Maschio, B. Kirtman, M. Rérat, R. Orlando, R. Dovesi, J. Chem. Phys. 2013, 139, 164102.
 DOI:10.1063/1.4824442
- C. M. Zicovich-Wilson, F. Pascale, C. Roetti, V. R. Saunders,
 R. Orlando, R. Dovesi, J. Comput. Chem. 2004, 25, 1873–1881. DOI:10.1002/jcc.20120
- F. Pascale, C. M. Zicovich-Wilson, F. López Gejo, B. Civalleri,
 R. Orlando, R. Dovesi, J. Comput. Chem. 2004, 25, 888–897.
 DOI:10.1002/jcc.20019
- 42. "CRYSPLOT A modern and easy to use visualization environment for plotting properties of crystalline solids as computed by means of the CRYSTAL code," can be found under http://crysplot.crystalsolutions.eu/index.html, 2022.

Povzetek

DOI:10.1002/zaac.202000181

V prispevku opisujemo spojini $[NMe_4][(BrF_5)_6(HF_2)]$ in $Cs_2[(BrF_5)_6(HF_2)(H_2F_3)]$, ki predstavljata prva primera kokristalov med BrF_5 in HF_2^- solmi. Ti spojini nastaneta pri reakcijah med BrF_5 in virom fluoridnih ionov, kot sta $[NMe_4]F$ ali CsF, ob prisotnosti vodikovega fluorida. Opis kristalnih struktur obeh spojin dopolnjujemo s kvantno kemijskimi izračuni trdne snovi in Ramansko spektroskopsko študijo spojine $[NMe_4][(BrF_5)_6(HF_2)]$. Kokristali vsebujejo diskretne $[HF_2]^-$ in $[H_2F_3]^-$ anione, ki so preko mostovnih F atomov koordinirani z molekulami BrF_5 . Kot ponavljajoči se strukturni motiv v teh spojinah se pojavlja propelerski način koordinacije F atoma s tremi molekulami BrF_5 , kot je bil že opažen v strukturi aniona $[Br_3F_{16}]^-$.



Except when otherwise noted, articles in this journal are published under the terms and conditions of the Creative Commons Attribution 4.0 International License